



REVIEW



Annexin A8 promotes VEGF-A driven endothelial cell sprouting

Nicole Heitzig ^a, Benjamin F. Brinkmann^a, Sophia N. Koerdt ^a, Gonzalo Rosso^b, Victor Shahin^b, and Ursula Rescher^a

^aInstitute of Medical Biochemistry, Center for Molecular Biology of Inflammation, and Interdisciplinary Clinical Research Center, University of Münster, Münster, Germany; ^bInstitute of Physiology II, University of Münster, Münster, Germany

ABSTRACT

The physiological and pathological process of angiogenesis relies on orchestrated endothelial cell (EC) adhesion, migration and formation of new vessels. Here we report that human umbilical vein endothelial cells (HUVECs) deficient in Annexin A8 (AnxA8), a member of the annexin family of Ca²⁺- and membrane binding proteins, are strongly deficient in their ability to sprout in response to vascular endothelial growth factor (VEGF)-A, and are strongly impaired in their ability to migrate and adhere to β 1 integrin-binding extracellular matrix (ECM) proteins. We find that these cells are defective in the formation of complexes containing the tetraspanin CD63, the main VEGF-A receptor VEGFR2, and the β 1 integrin subunit, on the cell surface. We observe that upon VEGF-A activation of AnxA8-depleted HUVECs, VEGFR2 internalization is reduced, phosphorylation of VEGFR2 is increased, and the spatial distribution of Tyr577-phosphorylated focal adhesion kinase (pFAK577) is altered. We conclude that AnxA8 affects CD63/VEGFR2/ β 1 integrin complex formation, leading to hyperactivation of the VEGF-A signal transduction pathway, and severely disturbed VEGF-A-driven angiogenic sprouting.

ARTICLE HISTORY

Received 3 October 2016
Revised 18 November 2016
Accepted 21 November 2016

KEYWORDS

angiogenesis; Annexin A8; β 1 integrin; CD63; endothelial cell sprouting; HUVEC; invasion; proximity ligation assay; tetraspanin; VEGFR2

Introduction


The formation of new blood vessels is an essential physiological requirement in development and wound repair. However, it is also a central mechanism in various pathophysiological conditions, such as cancer, and therefore might serve as a therapeutic target for the treatment. Angiogenesis proceeds via a series of sequential steps, among them adhesion, proliferation, migration and initiation of endothelial cell (EC) sprouts.^{1–3} These processes are controlled and coordinated by numerous intracellular signaling pathways that are initiated at the cell surface by functional complexes containing receptors and extracellular matrix-binding proteins.⁴ Vascular endothelial growth factor receptor 2 (VEGFR2), also known as KDR (kinase insert domain receptor), is highly expressed in angiogenic ECs.^{5,6} VEGFR2 is phosphorylated by VEGF-A activation. The dimerization of this receptor is required, but not sufficient for its activation.^{7–9}

VEGF-mediated VEGFR2 activation plays a crucial role in the initiation and orientation of sprouting by the recruitment of the transmembrane proteins like β 1 integrin into a functional macromolecular complex.^{3,5,10}

Cross-talk between VEGFR2 and β 1 integrin is important for adhesion to the extracellular matrix proteins. The entire higher order complex is assembled and stabilized by interaction with CD63, a member of the tetraspanin family of transmembrane proteins. CD63 is mainly present on internal vesicles of late endosomes (LE) and lysosomes¹¹ and serves as a widely used marker for these compartments. In ECs, it also localizes to Weibel-Palade bodies (WPB), from where it cycles to the plasma membrane (PM) via a mechanism that remains to be elucidated in detail.^{12,13} Based on our previous findings that Annexin A8 (AnxA8) is a crucial factor in CD63 cell surface presentation,¹⁴ we hypothesized that this protein might also regulate VEGFR2-driven angiogenesis. AnxA8 belongs to the highly conserved annexin protein family of Ca²⁺ and phospholipid-binding proteins.¹⁵ Annexins have been associated with a wide variety of cellular processes relevant for physiological and pathophysiological processes, such as proliferation, differentiation, migration, and inflammatory scenarios.^{16–18} AnxA8 has been shown to affect trafficking, morphology and distribution of LEs.^{19,20} Importantly, AnxA8 has been

CONTACT Ursula Rescher  rescher@uni-muenster.de  Institute of Medical Biochemistry, Centre for Molecular Biology of Inflammation, University of Münster, 48149 Münster, Germany.

Color versions of one or more of the figures in the article can be found online at www.tandfonline.com/kcam.

 Supplemental data for this article can be accessed on the publisher's website.

reported to affect leukocyte recruitment to activated endothelial cells due to mislocalization of CD63.¹⁴

Here we show that AnxA8 helps to establish functional plasma membrane hubs containing fully activated VEGFR2 in human umbilical vein endothelial cells (HUVECs), thereby exerting a pivotal role in regulation of VEGF-A-driven angiogenic sprouting.

Results

To investigate a potential role of AnxA8 in vessel formation, we assessed the angiogenic potential of HUVECs lacking AnxA8 in an in vitro-sprouting assay. To abolish AnxA8 expression, cells were transfected with constructs encoding either AnxA8-targeting or non-targeting shRNA and marking transfected cells by GFP expression. Immunoblot analysis showed a robust reduction of AnxA8 at the protein level to approximately 50% of control level (supplementary Fig. S1). To check for the specificity of the RNAi, we examined the expression level of the closely related protein AnxA1 and found no changes in its expression level (data not shown).

AnxA8 deficient HUVECs exhibit defective sprouting angiogenesis, migration and adhesion

For the sprouting assay, HUVECs were seeded onto microcarrier beads embedded in a 3-dimensional fibrinogen gel containing VEGF-A. Cells transfected with non-targeting control shRNA formed several clearly visible sprouts over the time course observed, with the first detectable sprouts appearing after 6–8 h (Fig. 1a). In stark contrast, loss of AnxA8 expression severely impaired sprouting, and the shRNA transfected cells remained in close contact with the microcarrier.

Further incubation of HUVECs up to 48 h after VEGF-A revealed that sprouting was not just delayed but profoundly disturbed (Fig. 1b). Although some cells lacking AnxA8 displayed delicate processes that penetrated the fibrin gel, very few cells were able to leave the microcarrier entirely, which was routinely observed for control cells. This phenotype was quantified by counting the number of cell nuclei that were visibly distanced from the bead after 48 h (Fig. 1b) and showed significantly impaired sprouting ability.

To rule out that AnxA8 deficiency might impact cell survival and proliferation, we assayed the cell numbers up to 72 h after siRNA and shRNA transfection (Fig. 1c). We did not detect differences in proliferation of AnxA8-silenced as compared with control cells. We therefore conclude that silencing of AnxA8 reduces sprouting propensity of HUVECs and that the observed sprouting

defect was not due to reduced cell division or enhanced apoptosis.

We next wanted to assess whether the sprouting defect was due to reduced cellular migration or adhesion, both of which are essential to angiogenesis. We first asked whether the defective sprouting seen in AnxA8-depleted cells was accompanied by a defective migratory capacity in a 3D-matrix. To address this, we monitored the ability of AnxA8-silenced cells to migrate across a Matrigel barrier in a VEGF-A-driven invasion assay. HUVECs downregulated in AnxA8 expression were severely impaired in their VEGF-A-stimulated invasive capacity (Fig. 2a), and statistical evaluation revealed that the differences were significant (Fig. 2b). We next investigated whether a change in the formation of adhesive contacts between the endothelial cells and the extracellular matrix was associated with the impaired angiogenesis and endothelial migration observed upon knockdown of AnxA8. Endothelial cell adhesion to the extracellular matrix (ECM) is mediated through binding of cell-surface receptors to ECM proteins. Because integrins constitute the major cell adhesion receptors, we aimed to analyze the impact of AnxA8 on integrin-mediated adhesion. Integrins are heterodimers containing an α and a β subunit, and vary in their affinities toward the different ECM proteins.²¹ Endothelial cells establish contacts to both fibrinogen, the ECM protein used in the sprouting assay, and Matrigel, a complex ECM protein mixture, via integrins containing the $\beta 1$ or the $\beta 3$ subunit.^{22,23} In contrast, vitronectin is rarely recognized by $\beta 1$ and preferentially engages $\beta 3$ integrins as receptors.²⁴

To analyze the integrin-dependent spreading ability of AnxA8-depleted HUVECs, we included the ECM proteins collagen type 1, fibronectin, and vitronectin. Collagen type 1 is a ligand for $\beta 1$ integrins,^{25,26} fibronectin is recognized by $\beta 1$ and $\beta 3$ integrins.^{22,23} Cells were tested for their ability to adhere to the different ECM proteins for 30 min. As shown in Fig. 2c, control cells adhered readily when tested on collagen type 1 and fibronectin substrates, whereas cells depleted in AnxA8 were less firmly attached to the substrates. However, adhesion seemed undisturbed on vitronectin (Fig. 2c). To Quantification and statistical evaluation of the adhesion behavior confirmed that AnxA8-depleted cells adhered significantly less strongly to the ECM proteins that bind to $\beta 1$ integrin, whereas $\beta 3$ integrin-mediated adhesion on vitronectin was only marginally affected (Fig. 2d), arguing for a defect primarily in integrin $\beta 1$ -mediated cell adhesion. Control cells adopted a well-spread morphology, whereas AnxA8-depleted cells covered a smaller spreading area on collagen and fibronectin. To characterize the altered spreading in a more quantitative manner, we analyzed the mean diameters of cells

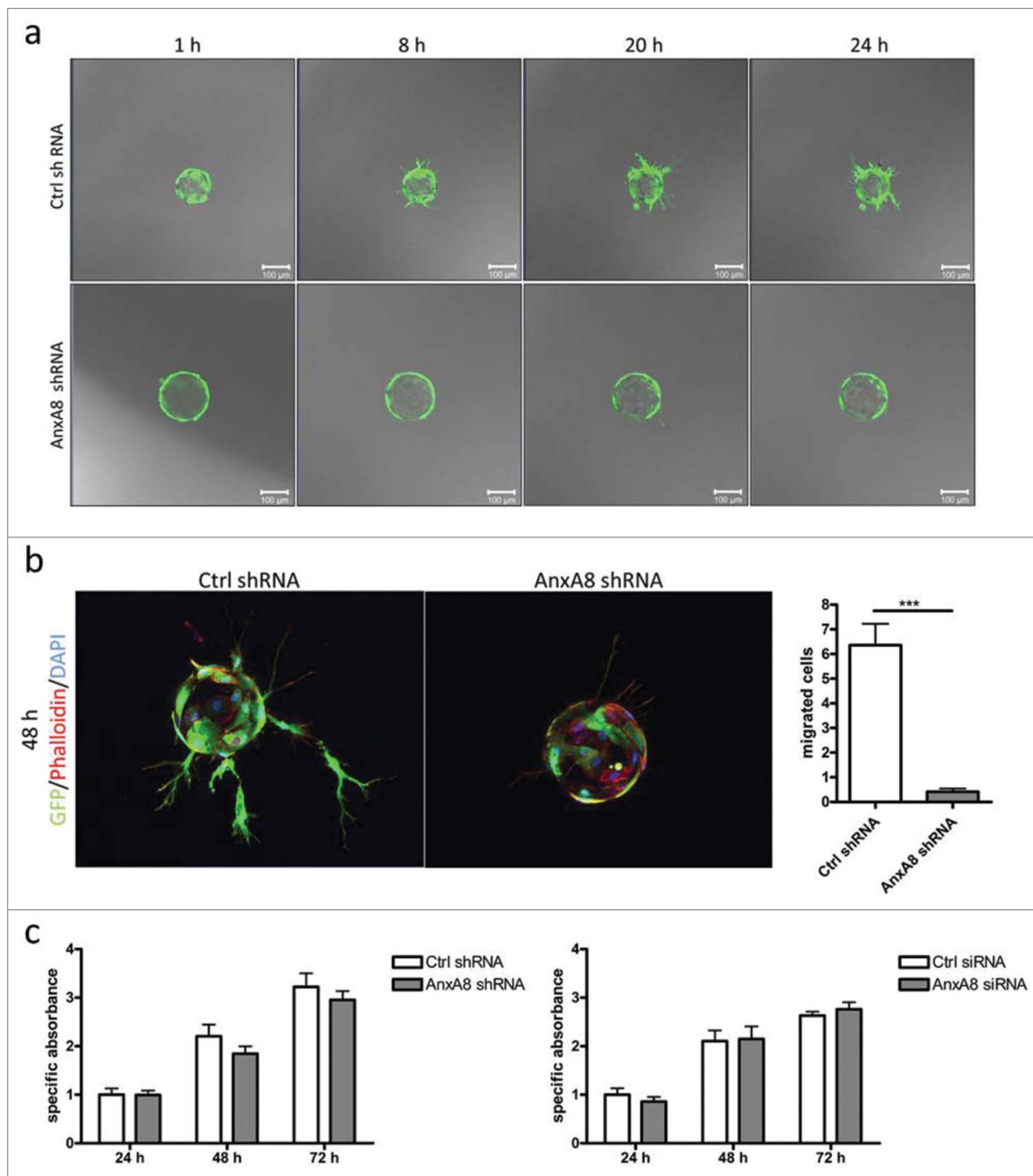


Figure 1. AnxA8 deficient HUVECs exhibit defective sprouting angiogenesis. (a) HUVECs transduced with non-targeting shRNA (Ctrl shRNA) or AnxA8-specific shRNA (AnxA8 shRNA) were cultured on microcarrier beads, embedded in 3D fibrinogen gels, and treated with 20 ng/ml VEGF-A. Spheroids were monitored by live cell microscopy in intervals of 30 min for 24 h. Stills of the respective time points are shown. Scale bars, 100 μ m (b) After 48 h of VEGF-A exposure, HUVECs were fixed, F-actin was stained with TRITC-phalloidin and DAPI was used to label DNA. To quantify the sprouting, confocal Z-stacks from at least 28 HUVEC spheroids/condition were taken, and nuclei of migrated cells (defined as cells not attached to the carrier bead) were counted. *** $P < 0.001$, unpaired Student's t -test, data represent means \pm SEM (c) Cell proliferation was analyzed after 24, 48 and 72 h. Data represent means \pm SEM of at least 6 independent experiments.

attached to the $\beta 1$ ligand collagen and found that AnxA8-depleted cells displayed significantly reduced mean diameters (Fig. 2e). Taken together, these results suggest that AnxA8 might be critically involved in the VEGF-A-driven adhesion, migration and sprouting of endothelial cells, caused by a defect in $\beta 1$ integrin-mediated cell-substrate adhesion.

AnxA8 depletion does not alter levels of total and cell surface-associated $\beta 1$ integrin and VEGFR2, but impairs CD63/VEGFR2/ $\beta 1$ integrin complex formation

Based on our results, we suspected that AnxA8 might impact proper cell surface presentation of $\beta 1$ integrin

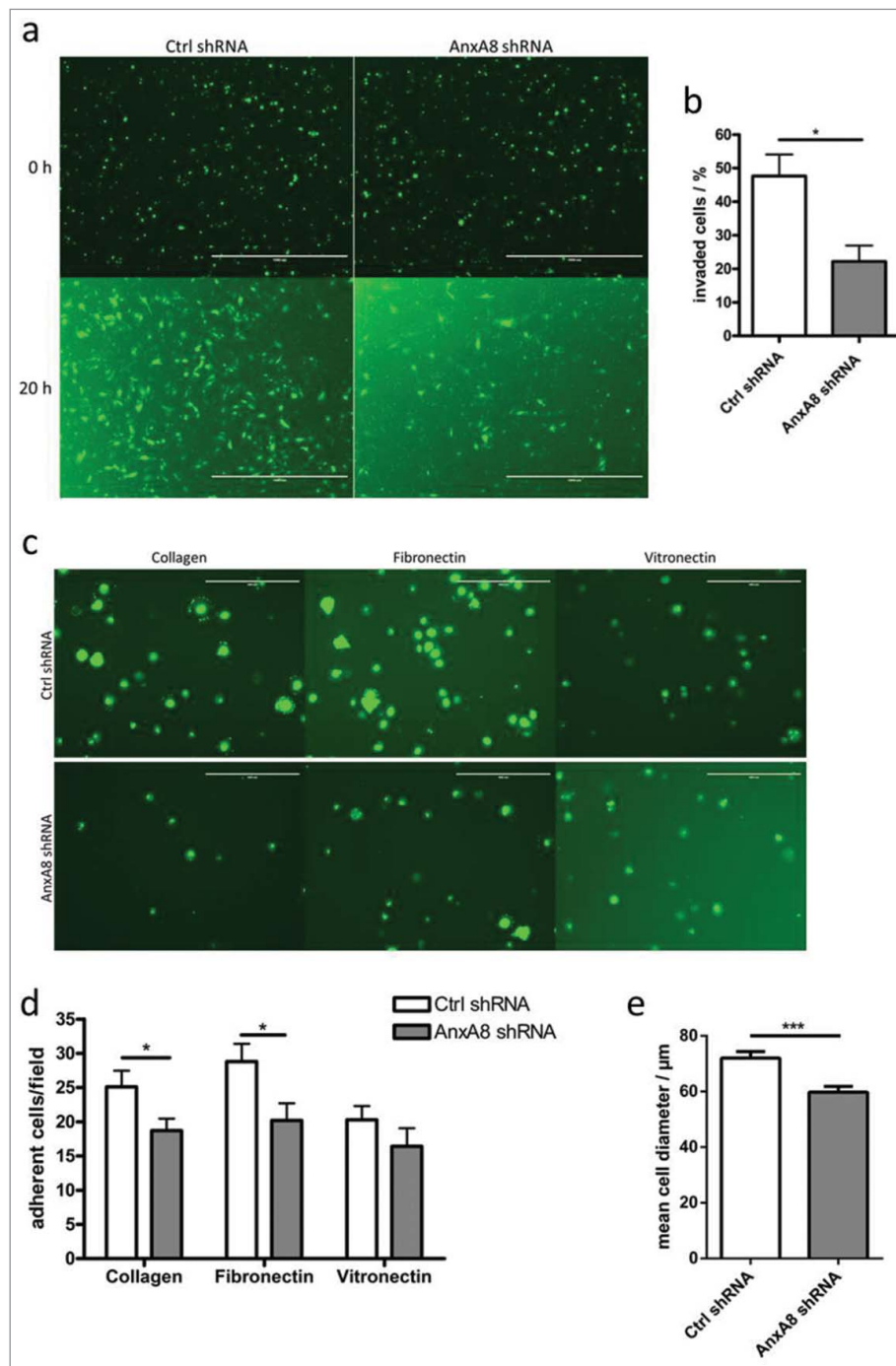


Figure 2. AnxA8 deficient HUVECs are impaired in migration and adhesion. (a) HUVECs treated with Ctrl or AnxA8 shRNA were seeded onto a matrigel-coated porous membrane and were allowed to migrate toward VEGF-A for 20 h. (b) To quantify the invasion capacity, the number of GFP-expressing cells on the lower side of the membrane was calculated as percentage of GFP-expressing cells on the upper side at time point 0. $*P < 0.05$, unpaired Student's *t*-test, data represent means \pm SEM of 4 independent experiments. Scale bars, 1 mm (c) Ctrl shRNA and AnxA8 shRNA transduced HUVECs were seeded onto collagen, fibronectin or vitronectin coated 96-well plates. (d) Adherent cells were fixed after 30 min and fluorescence images were taken. Number of cells was counted. $*P < 0.05$, unpaired Student's *t*-test, data represent means \pm SEM of 10 independent experiments. Scale bars, 400 μm . (e) HUVECs lentivirally transduced with either Ctrl shRNA or AnxA8 shRNA were seeded onto collagen-coated coverslips for 30 min. The mean diameters of the cells were analyzed by measuring cell lengths and widths. $***P < 0.001$, unpaired Student's *t*-test, data represent means \pm SEM of 40 cells of 4 independent experiments.

heterodimers, which are functionally activated upon VEGF-A stimulation of HUVECs.¹⁸ We therefore determined both the $\beta 1$ subunit expression levels in HUVEC

lysates and the $\beta 1$ subunit pool presented on the cell surface. As shown in Fig. 3a, quantification of the total $\beta 1$ subunit content revealed no differences between AnxA8

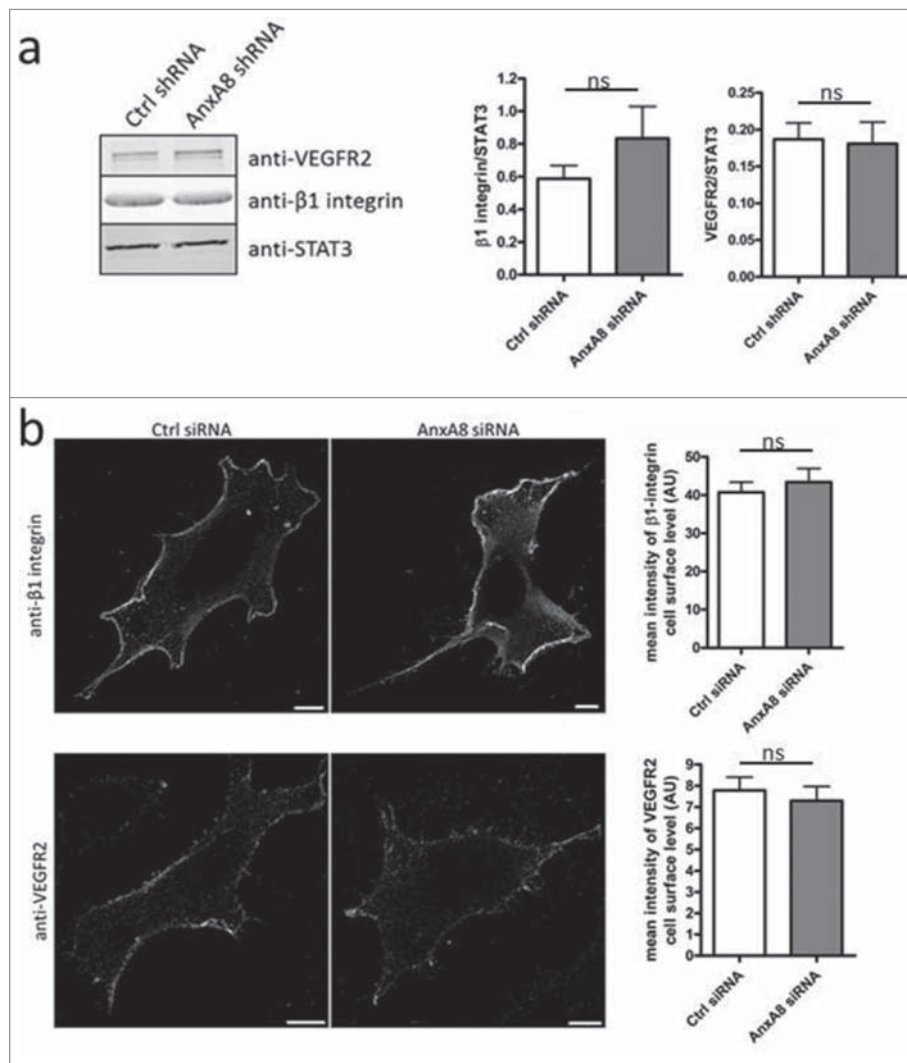


Figure 3. AnxA8 depleted HUVECs present the same levels of total and cell surface-associated $\beta 1$ integrin and VEGFR2. (a) Expression levels of $\beta 1$ integrin and VEGFR2 in lysates of control and AnxA8 silenced HUVECs were analyzed by immunoblotting. STAT3 served as a control for equal loading. Ratios of $\beta 1$ integrin or VEGFR2 versus STAT3 bands were quantified. $nsP > 0.05$, unpaired students t-test, data represent means \pm SEM of 7 independent experiments (b) Cell surface levels of $\beta 1$ integrin and VEGFR2 were analyzed by confocal microscopy. $nsP > 0.05$, unpaired Student's *t*-test, data represent means \pm SEM of at least 54 cells ($\beta 1$ integrin) of 4 independent experiments or 72 cells (VEGFR2) of 5 independent experiments. Scale bars, 10 μm .

knockdown and control cells, and no differences were observed when $\beta 1$ integrin subunit cell surface presentation was analyzed by single cell analysis (Fig. 3b).

VEGF-A-mediated endothelial adhesion, migration and angiogenesis are thought to depend on ligation of the VEGF-A receptor VEGFR2. Because VEGFR2 is complexed with $\beta 1$ integrin on the HUVEC surface¹⁰ we next determined whether VEGFR2 expression was affected in AnxA8-depleted cells. Similar to what we observed for $\beta 1$ integrin subunit expression, we did not detect alterations in the total VEGFR2 content (Fig. 3a) or in the levels of VEGFR2 cell surface pools (Fig. 3b).

We had shown previously that AnxA8 controls cell surface presentation of the tetraspanin CD63 in

HUVECs.¹⁴ Most importantly, CD63 is known to associate with both $\beta 1$ integrin and VEGFR2, keeping them in close proximity.¹ We therefore reasoned that although the respective cell surface levels were not affected, disturbed CD63/VEGFR2/ $\beta 1$ integrin complex formation might cause the defective adhesion and sprouting observed in AnxA8-silenced cells. To specifically visualize CD63/VEGFR2/ $\beta 1$ integrin interactions on the cell surface, we utilized the proximity ligation assay (PLA). In this approach, oligonucleotide-coupled antibodies are used to detect the potential interaction partners. Only when their targets are in close proximity (less than 40 nm), rolling circle amplification is initiated, giving rise to fluorescent spots. As shown in Fig. 4a, PLA signals were detected when control cells were treated with

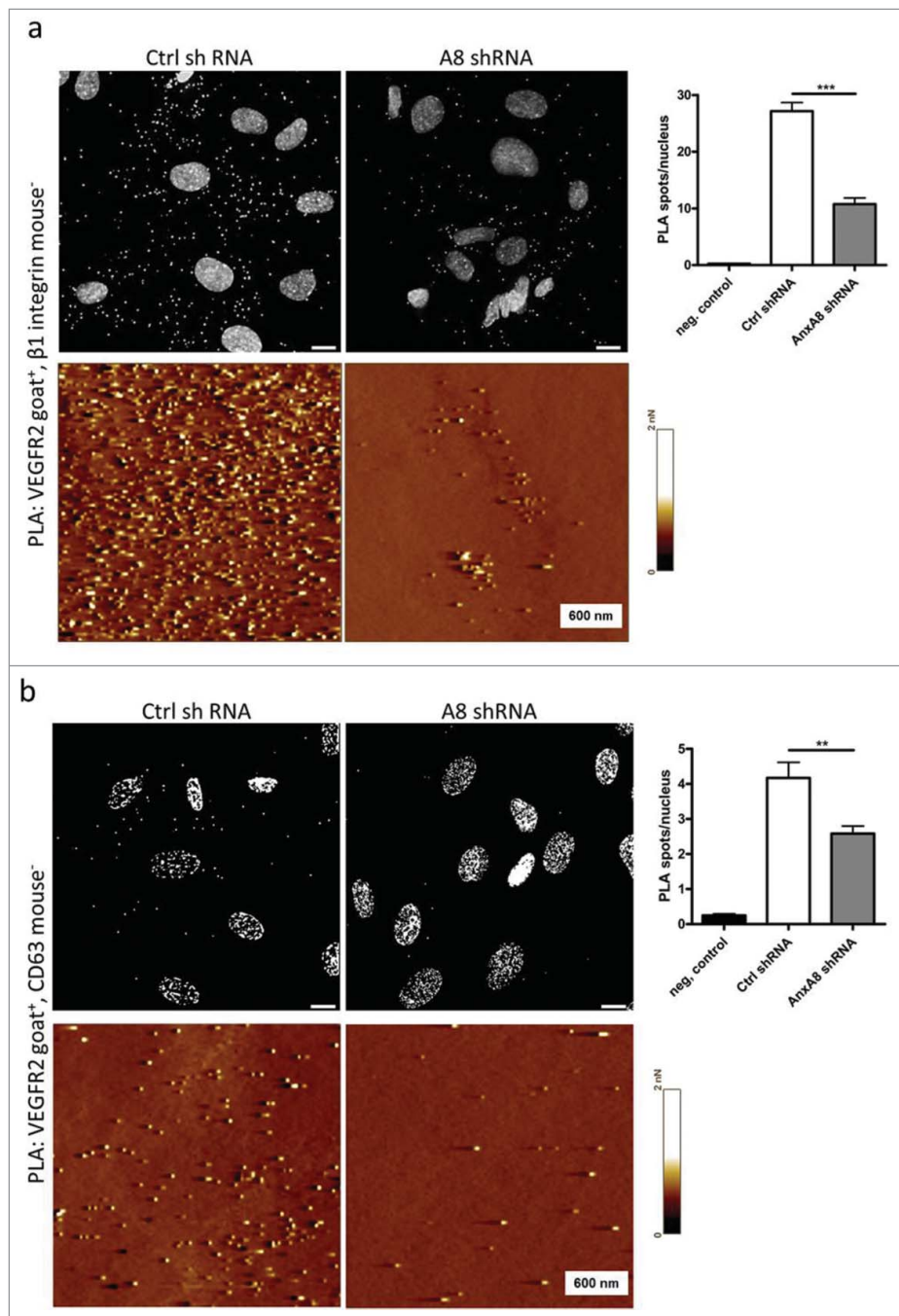


Figure 4. AnxA8 depletion impairs the CD63/VEGFR2/ β 1 integrin complex formation. HUVECs transduced with control or AnxA8 specific shRNA (identified by their green fluorescence) were analyzed for PLA signals representing complexes between (a) β 1 integrin/VEGFR2 and (b) CD63/VEGFR2 by confocal microscopy (upper panels) or atomic force microscopy (lower panels). For quantitative analysis, PLA spots per cell were calculated from confocal microscopy images. Means \pm SEM, $n = 48$ stacks of 4 independent experiments, student's t -test, *** $P < 0.001$, ** $P < 0.01$, scale bars, 10 μ m; AFM images, 600 nm.

anti-VEGFR2 and anti- β 1 integrin antibodies (Fig. 4a, upper panel) or anti-VEGFR2 and anti-CD63 antibodies (Fig. 4b, upper panel), confirming that VEGFR2, CD63, and β 1 integrin are present in a complex in resting cells. Silencing of AnxA8 resulted in a marked decrease of PLA signals, and quantitative analysis confirmed that the

differences were statistically significant (Fig. 4a, b). To investigate the heteromolecular complexes at higher resolution, we combined PLA with atomic force microscopy (AFM), thus obtaining topographical representation of the cell surface decorated with PLA signals. AnxA8-deficient cells consistently presented fewer globular

structures than control cells (Fig. 4a, b, lower panels), suggesting that the formation of CD63/VEGFR2/ β 1 integrin complexes is reduced in AnxA8-silenced cells.

VEGF-A signaling pathway is hyperactivated in AnxA8 deficient HUVECs

Because VEGFR2 signaling is altered depending on the association with integrin,¹⁰ we next focused on the VEGF-A-driven VEGFR2 signaling pathway. (Fig. 5a) and compared activation of VEGFR2 in the lysates of VEGF-A-stimulated control and AnxA8-depleted cells. Surprisingly, we detected significantly elevated phosphorylation levels at VEGFR2 autophosphorylation site1175 in the AnxA8-deficient HUVECs (Fig. 5b). Quantitative analysis of total VEGFR2 contents revealed a statistically significant reduction upon 30 min of VEGF-A exposure in control cells, whereas VEGFR2 levels were not significantly reduced in AnxA8-depleted cells (Fig. 5c). Because depletion of AnxA8 was not associated with elevated VEGFR2 levels (see above), and because p1175-VEGFR2/total VEGFR2 ratios were not affected (Fig. 5d), we suspected that hyperactivation of the VEGF-A-mediated signaling pathway was caused by impaired internalization of the activated receptor. We therefore analyzed cell surface presentation of VEGFR2 upon VEGF-A challenge and found that in AnxA8-depleted cells, VEGFR2 internalization was delayed. Quantitative analysis revealed a clear loss in VEGFR2 cell surface levels of control cells after 15 min of VEGF stimulation, whereas AnxA8-depleted cells, VEGFR2 levels were significantly higher at this time point (Fig. 5e), most likely increasing downstream signaling in response to VEGF-A. Growth factors promote phosphorylation of FAK, a non-receptor protein tyrosine kinase that associates with integrins at sites of focal adhesions and regulates assembly/disassembly of focal contacts.^{28,29} We therefore determined FAK phosphorylation at Tyr577, a site that lies in the FAK kinase domain and is required for maximal activation. Surprisingly, p577-FAK/total FAK ratios were not altered in AnxA8-silenced cells. However, the p577-FAK spatial distribution was profoundly changed. In control cells, p577-FAK localized to focal contacts along the cell periphery, whereas AnxA8-deficient cells displayed a more scattered pattern (Fig. 5g). In line with the above findings, quantification of p577-FAK signal intensities in situ revealed that activation per se was not affected (Fig. 5h).

Discussion

In this work, we show that AnxA8 impacts β 1 integrin-dependent endothelial cell adhesion and VEGF-A-

mediated sprouting. Expression levels of this annexin are rather low compared with other annexins present in HUVECs, and a 50% decrease in the amount of AnxA8 protein seems sufficient to fall below the critical threshold level, i.e. the manifestation of a mutant phenotype. We observed that AnxA8-depleted HUVECs displayed normal levels of the main endothelial VEGF receptor VEGFR2 and the integrin subunit β 1 on the cell surface. However, complex formation between the tetraspanin CD63 and VEGFR2, as well as VEGFR2 and integrin β 1 severely reduced. Although CD63 is a well-established marker for late endosomes and lysosomes¹¹ endothelial cells also present a significant pool on their surface.^{12,13,29} Cell surface-associated CD63 is part of the so-called tetraspanin web, a network of interactions of tetraspanins with each other and with unrelated surface molecules.³⁰ Interaction with CD63 on the plasma membrane seems to exert a regulatory function in the stabilization and endocytic trafficking of certain membrane proteins.^{31,32} We and others had shown previously that CD63 on HUVECs acts as a cofactor to P-selectin-mediated leukocyte recruitment onto the endothelial surface.^{12,14} Silencing of CD63 was reported to cause impaired leukocyte recruitment due to decreased P-selectin levels at the cell surface.¹² Most importantly, CD63 is known to associate with integrins containing the β 1 subunit³³ and VEGFR2.¹ Plasma membrane CD63 and late endosomal/lysosomal CD63 pools are connected. CD63 found within the multivesicular late endosomes cycles to the plasma membrane via the endothelium-specific, lysosomal-related Weibel-Palade bodies.^{13,35,36} We had found that the release of endosomal CD63 to replenish the PM levels is controlled by AnxA8, which affects the sorting of CD63 within the multivesicular endosomes. Consequently, CD63 is found retained on the intraluminal vesicle membrane in AnxA8-silenced HUVECs.¹⁴

The results presented in this study extend our previous findings and indicate that AnxA8-silenced cells display disturbed formation of another CD63-dependent functional complex on the cell surface. In contrast to P-selectin, which is constitutively internalized when not stabilized by CD63, we did not see differences in the cell surface expression of VEGFR2 and β 1, arguing for a role of CD63 in the assembly of a functional hub in which co-operating molecules are clustered and kept in close proximity. Interference with hub assembly might cause the defective adhesion and sprouting observed in AnxA8-silenced cells. In support of our model, knock-down of CD63 in HUVECs results in disturbed angiogenic sprouting and adhesion.¹ However, the phenotype appears more severe, with reduced adhesion also on the β 3 integrin-engaging ECM protein vitronectin. This might be explained by the observation that in resting

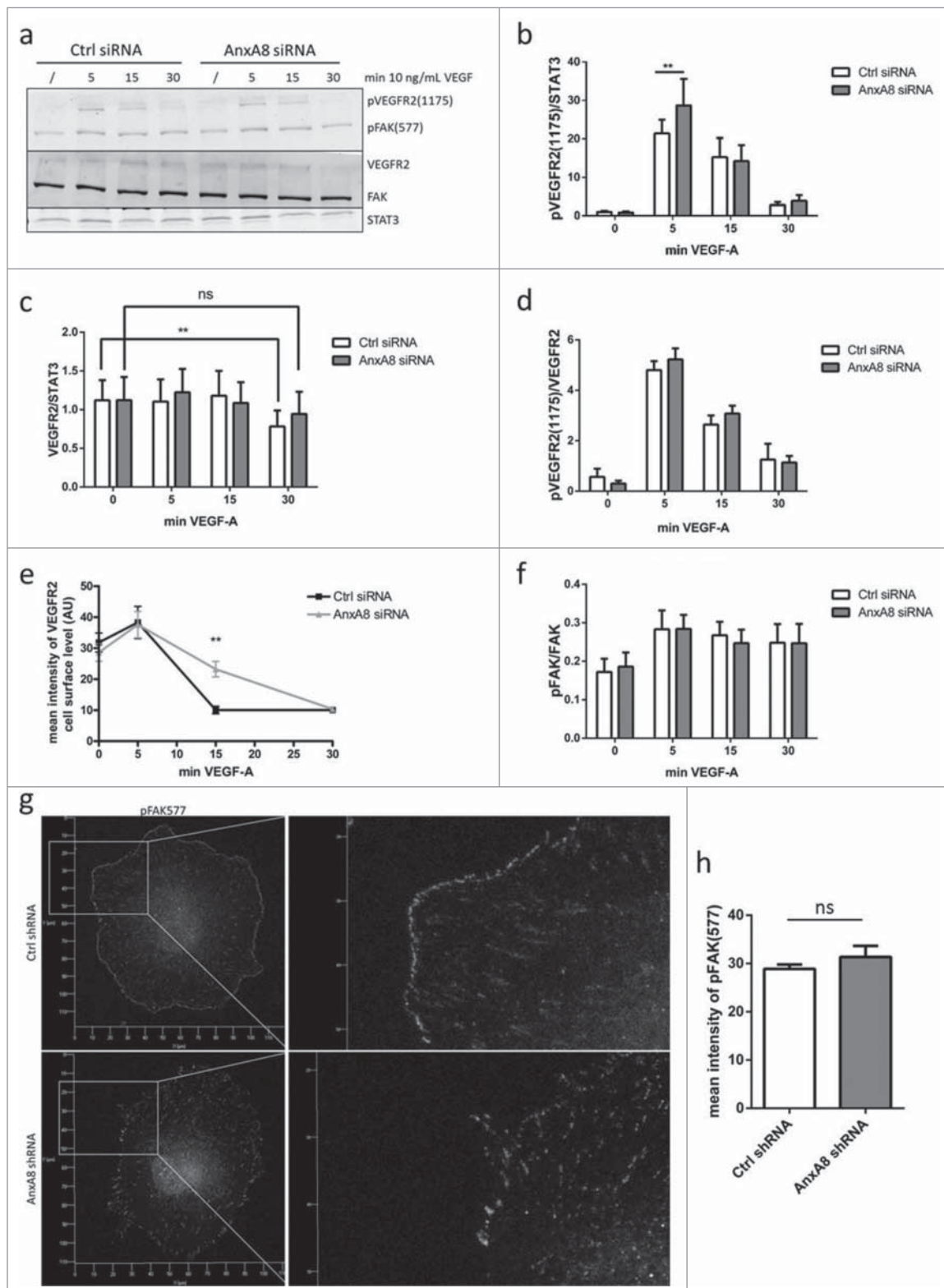


Figure 5. (For figure legend, see page 283)

HUVECs, CD63 is also associated with $\beta 3$ integrin, although to a lesser extent.^{1,37} Yet, we do not know about the stability of the CD63/integrin-based functional hubs. While transiently lowering the CD63 content in the

plasma membrane, e. g. by silencing of AnxA8, might affect the formation of more dynamic signaling complexes, more stable, longer-lasting interactions with CD63 might not be affected and might only be interfered

with when CD63 is ablated. A shift toward $\beta 3$ integrin-based focal contacts might also explain the altered FAK distribution pattern observed in AnxA8 silenced cells, as FAK has been shown to associate with both $\beta 1$ and $\beta 3$ integrins in HUVECs.³⁶ Interestingly and similar to CD63 KO mice,³⁹ AnxA8 KO mice are viable and do not display an overt vascular phenotype.¹⁴ In particular, they neither suffer from embryonic lethality, or birth defects. Although it cannot be ruled out that other annexins or tetraspanins might compensate for the respective loss of AnxA8 or CD63, it is highly likely that AnxA8 and CD63 are not involved in developmental angiogenesis but rather control endothelial migration/invasion in more pathophysiological settings such as wound healing or tumor-driven angiogenesis.

Angiogenesis, and the neovascularization of tumors, is critically dependent on cross-talk between and integration of VEGF-mediated signaling pathways and integrins.^{6,25,26,40} While the dynamic nature of integrins and their constant cycling to and from the plasma membrane via endosomal pathways is well acknowledged,^{41,42,43} a growing body of evidence suggests that they might also be transferred to late endosomes to be either degraded or transported back to the cell surface,^{44,45} and re-directing integrins to other endosomal pathways might contribute to aberrant cell migration and invasion, as seen in cancer progression.⁴⁶ These trafficking steps directly affect the level of integrins at the PM. In contrast to this, interfering with the assembly of at least $\beta 1$ integrin in a complex with CD63 and VEGFR2 does not alter the amount of $\beta 1$ integrin (see above, and¹). Furthermore, binding to CD63 is not needed for $\beta 1$ integrin to adopt the active state.¹ However, the defective adhesion on $\beta 1$ integrin-binding ECM proteins strongly argues for a decisive function of the integrin-containing macromolecular complexes. Clearly, the assembly of functionally co-operating signaling molecules into a functional complex exhibits multiplicative effects due to synchronous action between neighboring molecules. Whereas in unstimulated HUVECs, VEGFR2 is mostly associated with $\beta 1$ integrin, (our work and ref. 1), VEGF stimulation favors

formation of a VEGFR2- $\beta 3$ integrin interaction and $\beta 3$ integrin phosphorylation.⁴⁰

Our data add to the complex and multi-step control of the interplay of growth factors and integrins and support a model in which AnxA8-dependent plasma membrane expression of CD63 establishes an additional layer of regulation to critically control major factors that mediate essential endothelial functions, such as angiogenesis.

Materials and methods

Antibodies and plasmids

Goat polyclonal anti-human Annexin A8 antibody (C-20), and polyclonal rabbit anti-FAK (C-20) were obtained from Santa Cruz, mouse monoclonal anti-CD63 antibody was from the Developmental Studies Hybridoma Bank (clone H5C6, University of Iowa, Iowa City, IA, USA). Rabbit anti-phospho-FAK(577) antibody, monoclonal rabbit anti-pVEGFR2(1175) antibody, and rabbit polyclonal anti-STAT3 antibodies were purchased from Cell Signaling. Goat anti-VEGFR2 antibodies (AF357) were obtained from R&D System, monoclonal mouse anti- $\beta 1$ integrin (MAP1965) was from Millipore. Plasmids psPAX2 (Addgene plasmid #12260) and pMD2.G (Addgene plasmid #12259) were gifts from Didier Trono, HuShRNA plasmids pGFP-C-shLenti non-targeting Ctrl shRNA (TR30021), and AnxA8-silencing shRNA (TL314B) were from OriGen.

Isolation and culture of Human umbilical vein endothelial cells (HUVECs)

HUVECs were isolated from umbilical cords by dispase treatment and cultured on CellBind Surface dishes (Corning) or on collagen type 1-coated coverslips in supplement-containing EGM2 (Promocell) or in HUVEC-Mix medium composed of 50% EGM2 with supplements and 50% M199 (Biochrom) supplemented with 10% fetal calf serum (Sigma), 30 $\mu\text{g}/\text{mL}$ gentamycin (Cytogen), 15 ng/mL amphotericin B (Biochrom), 100 IE Heparin

Figure 5. (see previous page) VEGF-A signaling pathway is hyperactivated in AnxA8 deficient HUVECs. HUVECs transfected with non-targeting siRNA (Ctrl siRNA) or AnxA8-specific siRNA (AnxA8 siRNA) were exposed to VEGF-A for the indicated periods of time. (a) Cell lysates were immunoblotted for the amount and activation state of downstream signaling components (respective phospho-sites analyzed are given in brackets). STAT3 was used as a loading control. Levels of (b) VEGFR2 activation at autophosphorylation site 1175 and (c) total VEGFR2 were quantified as ratios of pVEGFR(1175) or total VEGFR2 vs. STAT3 levels in the lysates. $**P < 0.01$, nsP > 0.05, data represent means \pm SEM of 8 independent experiments and were analyzed by ANOVA followed by Fisher's LSD post-hoc test (d) Levels of pVEGFR2(1175) were quantified as ratios vs. total VEGFR2, data represent means \pm SEM of 8 independent experiments. (e) Specific cell surface levels of VEGFR2 after VEGF-A challenge were detected by immunofluorescence microscopy. $**P < 0.01$, data represent means \pm SEM of at least 42 cells of 3 independent experiments and were analyzed by unpaired student's *t*-test. (f) Levels of pFAK(577) were quantified as ratios vs. total FAK, data represent means \pm SEM of 6 independent experiments. (g) HUVECs transduced with either Ctrl shRNA or AnxA8 shRNA were seeded onto collagen-coated coverslips for 30 min. (h) pFAK577 levels of the cells were analyzed by confocal microscopy. nsP > 0.05, unpaired Student's *t*-test, data represent means \pm SEM of 40 cells of 4 independent experiments.

(Ratiopharm), 2 mM L-glutamine (Lonza) at 5% CO₂ and 37°C. All work with HUVECs was conducted with the formal approval of the Ethics Committee of North Rhine-Westphalia and the University of Münster.

HUVEC transfection

Cells were transfected with 400 pmol siRNA (AnxA8 siRNA 5'-GGAGCGGAGAUUGACUAAAAdTdT-3' or non-targeting Ctrl siRNA [AllStars negative control siRNA Qiagen]) using the Amaxa Nucleofection Technology (HUVEC Nucleofector Kit-OLD, Lonza) following the manufacturer's instruction, and cultured for 48 h. For lentiviral transduction, HUVECs were incubated overnight with the lentivirus-containing supernatant together with 4 µg/mL polybrene (Santa Cruz). HUVECs were cultured in supplemented EGM2 for 2 d before analysis.

Production of shRNA containing lentiviral particles

Lentiviral particles were produced in HEK293T cells cultured in DMEM (Sigma) with 10% fetal calf serum (Biocrom), 2 mM L-glutamine, 1% non-essential amino acid solution (Biocrom) and 100 U/mL penicillin and 100 µg/mL streptomycin (Lonza). Cells were co-transfected using Xfect Transfection Reagent (Clontech) with plasmids encoding both shRNA and GFP together with the packaging vectors psPAX2 and pMD2.G. After 24 h, the medium (DMEM) of the HEK293T cells was replaced with EGM2. After additional 24 h, the lentivirus particle-containing supernatant was harvested.

Cell proliferation assay

Proliferation assay with WST-1 reagent (Roche) was performed according to the manufacturer's protocol. After transfection/transduction, 2×10^4 HUVECs were seeded in duplicates on collagen-coated 96-Well plates for 24, 48 or 72 h. Cells were incubated with WST-1 reagent for 1 h. Absorbance was measured at 440 nm.

Western blotting

For western blotting analysis cells were directly lysed by incubation in lysis buffer (62.5 mM Tris pH 6.8, 10% glycerol, 5% β-mercaptoethanol, 4% sodium dodecyl sulfate, 0.002% bromophenol blue) on a shaker at 400 rpm for 4 h. Lysates were boiled up at 96°C for 10 min. Samples were loaded onto a 12% SDS PAGE and separated proteins were measured by means of near-infrared fluorescence detection (LI-COR Biosciences GmbH, Bad Homburg, Germany).

Microcarrier-based sprouting assay

Lentivirally transduced HUVECs were used for sprouting assay as previously described.⁴⁷ A fibrinogen solution together with HUVEC-loaded Cytodex 3 microcarrier beads (Sigma) were given to an 8 Well Glass Bottom µ-Slide (ibidi) and exposed to 20 ng/mL VEGF-A. After 48 h, cells were fixed with 4% paraformaldehyde (PFA) for 30 min, gently washed with glycine buffer (PBS²⁺, 100 mM glycine), blocked with blocking buffer (PBS²⁺, 10% FCS, 0.2% Triton X-100, 0.05% Tween 20, 0.02% BSA) for 1 h and incubated with TRITC-Phalloidin in blocking buffer overnight. Incubation with 1 mg/mL DAPI (Thermo Scientific) in PBS²⁺ was performed for 20 min.

Invasion assay

4×10^4 lentivirally transduced HUVECs were resuspended in serum-free M199 medium and added to the inserts of a 24-well BioCoat Invasion Chamber (Corning) with the upper surface of the insert membranes coated with growth factor reduced Matrigel. The lower compartment was filled with HUVEC-Mix medium containing 10 ng/mL VEGF-A. Images were taken at time point 0 h. The cells were allowed to pass through the matrix and the membrane pores for 20 h. HUVECs were washed with PBS⁺⁺ and the non-invaded cells were removed. The invaded cells at the bottom of the membrane were fixed with 4% PFA in PBS⁺⁺ for 10 min and the nuclei were stained with Hoechst33342 (20 mM; 1:500) in PBS⁺⁺ for 15 min. Cell invasion was documented microscopically. For each condition, the cells from 3 images were counted. Cells successfully transduced with shRNA were identified by their green fluorescence. The initial number of transfected cells in the upper compartment at time point 0 was set to 100% and the percentage of transfected cells on the bottom of the porous membrane was calculated at time point 20.

Adhesion assay

Transient transfected HUVECs were suspended in EGM2 medium containing 1% BSA and $5 \cdot 10^3$ cells were seeded on collagen, fibronectin or vitronectin-coated 96-well plates for 30 min. Cells were fixed with 4% PFA for 10 min and nuclei were stained with 1 µg/mL Hoechst33342. Adherent cells were documented in duplicates using an EVOS microscope (AMF) and number of attached cells/field was calculated.

Mean diameters of lentivirally transduced HUVECs seeded on collagen-coated coverslips for 30 min were analyzed by measuring cell length and width of the near-

spherical cells using the LSM 800 confocal microscope (Carl Zeiss) equipped with a Plan-Apochromat 63x/1.4 oil immersion objective.

Proximity ligation assay

HUEVCs were fixed with 4% PFA for 10 min and blocked with 2% BSA/PBS⁺⁺ for 15 min at room temperature. Samples were incubated with the primary antibodies for 1.5 h. Subsequently, the respective secondary antibodies were added for 1 h. Proximity ligation assay (PLA) was performed according to the manufacturer's instruction (Sigma, Duolink). PLA spots per nucleus were calculated using ImageJ software (NIH).

Live-cell imaging and confocal microscopy

Live Cell Microscopy was performed on a LSM 780 microscope (Carl Zeiss) with a 10x/air DICIII objective. Confocal imaging of fixed cells was performed using the LSM 780 microscope (Carl Zeiss) equipped with a Plan-Apochromat 63x/1.4 oil immersion objective.

Atomic force microscopy

For topographical investigations of the PLA complexes on the cell surface of lentiviral transduced HUVECs, a JPK Nanowizard 3 AFM system (JPK instruments) was employed. V-shaped OTR4 tips (Olympus) with a nominal spring constant of 0.02 Nm⁻¹ were used to image the cell surface in contact mode. During imaging acquisition, the force between the cantilever and the sample was adjusted manually to the lowest possible (generally ~50 pN) and feedback gains were optimized to achieve highest possible topographical resolution. HUVECs were fixed with 4% PFA for 20 minutes and imaged in fluid (PBS buffer) with 512 lines per screen. Line scan frequencies were between 1–1.5 Hz. Data were processed and analyzed with appropriate commercially available software (JPK SPM data Processing).

VEGF-A signaling and degradation

siRNA transfected serum-starved HUVECs were incubated with 10 ng/mL VEGF-A (PeproTech) for 0, 5, 15 or 30 min and directly lysed for immunoblotting or fixed with 4% PFA for 10 min. After blocking in 2% BSA in PBS, cells were incubated with anti-VEGFR2 antibodies for 1 h and Alexa Fluor 488 Donkey a-Goat IgG for 45 min at room temperature. DNA was stained with DAPI in PBS for 10 min.

Statistical analysis

The bars represent mean values ± SEM. Statistical significance of the results was evaluated by Student's unpaired t-test using GraphPad Prism version 4.0 (GraphPad software, San Diego, CA, USA). A p value < 0.05 was considered as statistically significant.

Disclosure of potential conflicts of interest

No potential conflicts of interest were disclosed.

Funding

This work was supported by funding to U.R. from the Interdisciplinary Clinical Research Center of the Münster Medical School (IZKF, RE2/026/15) and the German Research Foundation (DFG; SFB1009/A06, GRK1409).

Author contributions

N.H. designed and performed the experiments, collected and analyzed the data and wrote the manuscript. B.B. performed and analyzed the spheroid sprouting experiments. S.N.K. designed and performed acquisition and statistical analysis of images. G.R. and V.S. performed and analyzed the AFM experiments. U.R. supervised the research, analyzed the data and wrote the manuscript.

ORCID

Nicole Heitzig  <http://orcid.org/0000-0003-1710-0406>
Sophia N. Koerdt  <http://orcid.org/0000-0001-6392-8138>

References

- [1] Tugues S, Honjo S, König C, Padhan N, Kroon J, Gualandi L, Li X, Barkefors I, Thijssen VL, Griffioen AW, et al. Tetraspanin CD63 promotes vascular endothelial growth factor receptor 2- β 1 integrin complex formation, thereby regulating activation and downstream signaling in endothelial cells in vitro and in vivo. *J Biol Chem* 2013; 288:19060-71; PMID:23632027; <https://doi.org/10.1074/jbc.M113.468199>
- [2] Potente M, Gerhardt H, Carmeliet P. Basic and therapeutic aspects of angiogenesis. *Cell* 2011; 146:873-87; PMID:21925313; <https://doi.org/10.1016/j.cell.2011.08.039>
- [3] Eilken HM, Adams RH. Dynamics of endothelial cell behavior in sprouting angiogenesis. *Curr Opin Cell Biol* 2010; 22:617-25; PMID:20817428; <https://doi.org/10.1016/j.ceb.2010.08.010>
- [4] Ramjaun AR, Hodivala-Dilke K. The role of cell adhesion pathways in angiogenesis. *Int J Biochem Cell Biol* 2009; 41:521-30; PMID:18762270; <https://doi.org/10.1016/j.biocel.2008.05.030>
- [5] Koch S, Claesson-Welsh L. Signal transduction by vascular endothelial growth factor receptors. *Cold Spring Harb*

- Perspect Med.2012;2:a006502; PMID:22762016; <https://doi.org/10.1101/cshperspect.a006502>
- [6] Alitalo K, Tammela T, Petrova TV. Lymphangiogenesis in development and human disease. *Nature* 2005; 438 (7070):946-53; PMID:16355212; <https://doi.org/10.1038/nature04480>
- [7] Nilsson I, Bahram F, Li X, Gualandi L, Koch S, Jarvius M, Söderberg O, Anisimov A, Kholová I, Pytowski B, et al. VEGF receptor 2/–3 heterodimers detected in situ by proximity ligation on angiogenic sprouts. *EMBO J* 2010; 29:1377-88; PMID:20224550; <https://doi.org/10.1038/emboj.2010.30>
- [8] Dosch DD, Ballmer-Hofer K. Transmembrane domain-mediated orientation of receptor monomers in active VEGFR-2 dimers. *FASEB J Off Publ Fed Am Soc Exp Biol* 2010; 24:32-8
- [9] Stuttfeld E, Ballmer-Hofer K. Structure and function of VEGF receptors. *IUBMB Life* 2009; 61:915-22; PMID:19658168; <https://doi.org/10.1002/iub.234>
- [10] Chen TT, Luque A, Lee S, Anderson SM, Segura T, Iruela-Arispe ML. Anchorage of VEGF to the extracellular matrix conveys differential signaling responses to endothelial cells. *J Cell Biol* 2010; 188:595-609; PMID:20176926; <https://doi.org/10.1083/jcb.200906044>
- [11] Pols MS, Klumperman J. Trafficking and function of the tetraspanin CD63. *Exp Cell Res* 2009; 315:1584-92; PMID:18930046; <https://doi.org/10.1016/j.yexcr.2008.09.020>
- [12] Doyle EL, Ridger V, Ferraro F, Turmaine M, Saftig P, Cutler DF. CD63 is an essential cofactor to leukocyte recruitment by endothelial P-selectin. *Blood* 2011; 118:4265-73; PMID:21803846; <https://doi.org/10.1182/blood-2010-11-321489>
- [13] Vischer UM, Wagner DD. CD63 is a component of Weibel-Palade bodies of human endothelial cells. *Blood* 1993; 82:1184-91; PMID:8353283
- [14] Poeter M, Brandherm I, Rossaint J, Rosso G, Shahin V, Skryabin BV, Zarbock A, Gerke V, Rescher U. Annexin A8 controls leukocyte recruitment to activated endothelial cells via cell surface delivery of CD63. *Nat Commun* 2014; 5:3738; PMID:24769558; <https://doi.org/10.1038/ncomms4738>
- [15] Rescher U, Gerke V. Annexins—unique membrane binding proteins with diverse functions. *J Cell Sci* 2004; 117:2631-9; PMID:15169834; <https://doi.org/10.1242/jcs.01245>
- [16] Brandherm I, Disse J, Zeuschner D, Gerke V. cAMP-induced secretion of endothelial von Willebrand factor is regulated by a phosphorylation/dephosphorylation switch in annexin A2. *Blood* 2013; 122:1042-51; PMID:23757730; <https://doi.org/10.1182/blood-2012-12-475251>
- [17] Gerke V. Annexins A2 and A8 in endothelial cell exocytosis and the control of vascular homeostasis. *Biol Chem* 2016; 397:995-1003; PMID:27451994; <https://doi.org/10.1515/hsz-2016-0207>
- [18] Kuehnl A, Musiol A, Raabe CA, Rescher U. Emerging functions as host cell factors - an encyclopedia of annexin-pathogen interactions. *Biol Chem* 2016; 397:949-59; PMID:27366904; <https://doi.org/10.1515/hsz-2016-0183>
- [19] Goebeler V, Poeter M, Zeuschner D, Gerke V, Rescher U. Annexin A8 Regulates Late Endosome Organization and Function. *Mol Biol Cell* 2008; 19:5267-78; PMID:18923148; <https://doi.org/10.1091/mbc.E08-04-0383>
- [20] Goebeler V, Ruhe D, Gerke V, Rescher U. Annexin A8 displays unique phospholipid and F-actin binding properties. *FEBS Lett* 2006; 580:2430-4; PMID:16638567; <https://doi.org/10.1016/j.febslet.2006.03.076>
- [21] Margadant C, Monsuur HN, Norman JC, Sonnenberg A. Mechanisms of integrin activation and trafficking. *Curr Opin Cell Biol* 2011; 23:607-14; PMID:21924601; <https://doi.org/10.1016/jceb.2011.08.005>
- [22] Humphries JD, Byron A, Humphries MJ. Integrin ligands at a glance. *J Cell Sci* 2006; 119:3901-3; PMID:16988024; <https://doi.org/10.1242/jcs.03098>
- [23] Israels SJ, McMillan-Ward EM, Easton J, Robertson C, McNicol A. CD63 associates with the alphaIIb beta3 integrin-CD9 complex on the surface of activated platelets. *Thromb Haemost* 2001; 85:134-41; PMID:11204565
- [24] Horton MA. The alpha v beta 3 integrin “vitronectin receptor.” *Int J Biochem Cell Biol* 1997; 29:721-5; PMID:9251239; [https://doi.org/10.1016/S1357-2725\(96\)00155-0](https://doi.org/10.1016/S1357-2725(96)00155-0)
- [25] Senger DR, Claffey KP, Benes JE, Perruzzi CA, Sergiou AP, Detmar M. Angiogenesis promoted by vascular endothelial growth factor: regulation through alpha1-beta1 and alpha2beta1 integrins. *Proc Natl Acad Sci U S A* 1997; 94:13612-7; PMID:9391074; <https://doi.org/10.1073/pnas.94.25.13612>
- [26] Bloch W, Forsberg E, Lentini S, Brakebusch C, Martin K, Krell HW, Weidle UH, Addicks K, Fässler R. Beta 1 integrin is essential for teratoma growth and angiogenesis. *J Cell Biol* 1997; 139:265-78; PMID:9314545; <https://doi.org/10.1083/jcb.139.1.265>
- [27] Byzova TV, Goldman CK, Pampori N, Thomas KA, Bett A, Shattil SJ, Plow EF. A Mechanism for Modulation of Cellular Responses to VEGF: Activation of the Integrins. *Mol Cell* 2000; 6:851-60; PMID:11090623
- [28] Schlaepfer DD, Mitra SK, Ilic D. Control of motile and invasive cell phenotypes by focal adhesion kinase. *Biochim Biophys Acta* 2004; 1692:77-102; PMID:15246681; <https://doi.org/10.1016/j.bbamcr.2004.04.008>
- [29] Mitra SK, Hanson DA, Schlaepfer DD. Focal adhesion kinase: in command and control of cell motility. *Nat Rev Mol Cell Biol* 2005; 6:56-68; PMID:15688067; <https://doi.org/10.1038/nrm1549>
- [30] Hotta H, Ross AH, Huebner K, Isobe M, Wendeborn S, Chao MV, Ricciardi RP, Tsujimoto Y, Croce CM, Koprowski H. Molecular cloning and characterization of an antigen associated with early stages of melanoma tumor progression. *Cancer Res* 1988; 48:2955-62; PMID:3365686
- [31] Yunta M, Lazo PA. Tetraspanin proteins as organisers of membrane microdomains and signalling complexes. *Cell Signal* 2003; 15:559-64; PMID:12681443; [https://doi.org/10.1016/S0898-6568\(02\)00147-X](https://doi.org/10.1016/S0898-6568(02)00147-X)
- [32] Duffield A, Kamsteeg E-J, Brown AN, Pagel P, Caplan MJ. The tetraspanin CD63 enhances the internalization of the H,K-ATPase beta-subunit. *Proc Natl Acad Sci U S A* 2003; 100:15560-5; PMID:14660791; <https://doi.org/10.1073/pnas.2536699100>

- [33] Jung K-K, Liu X-W, Chirco R, Fridman R, Kim H-RC. Identification of CD63 as a tissue inhibitor of metalloproteinase-1 interacting cell surface protein. *EMBO J* 2006; 25:3934-42; PMID:16917503; <https://doi.org/10.1038/sj.emboj.7601281>
- [34] Mannion BA, Berditchevski F, Kraeft SK, Chen LB, Hemler ME. Transmembrane-4 superfamily proteins CD81 (TAPA-1), CD82, CD63, and CD53 specifically associated with integrin alpha 4 beta 1 (CD49d/CD29). *J Immunol Baltim Md* 1950 1996; 157:2039-47
- [35] Kobayashi T, Vischer UM, Rosnoblet C, Lebrand C, Lindsay M, Parton RG, Kruihof EK, Gruenberg J. The tetraspanin CD63/lamp3 cycles between endocytic and secretory compartments in human endothelial cells. *Mol Biol Cell* 2000; 11:1829-43; PMID:10793155; <https://doi.org/10.1091/mbc.11.5.1829>
- [36] Subramaniam M, Koedam JA, Wagner DD. Divergent fates of P- and E-selectins after their expression on the plasma membrane. *Mol Biol Cell* 1993; 4:791-801; PMID:7694691; <https://doi.org/10.1091/mbc.4.8.791>
- [37] Somanath PR, Malinin NL, Byzova TV. Cooperation between integrin alphavbeta3 and VEGFR2 in angiogenesis. *Angiogenesis* 2009; 12:177-85; PMID:19267251; <https://doi.org/10.1007/s10456-009-9141-9>
- [38] Eliceiri BP, Puente XS, Hood JD, Stupack DG, Schlaepfer DD, Huang XZ, Sheppard D, Cheresh DA. Src-mediated coupling of focal adhesion kinase to integrin $\alpha v \beta 5$ in vascular endothelial growth factor signaling. *J Cell Biol* 2002; 157:149-60; PMID:11927607; <https://doi.org/10.1083/jcb.200109079>
- [39] Schröder J, Lüllmann-Rauch R, Himmerkus N, Pleines I, Nieswandt B, Orinska Z, Koch-Nolte F, Schröder B, Bleich M, Saftig P. Deficiency of the tetraspanin CD63 associated with kidney pathology but normal lysosomal function. *Mol Cell Biol* 2009; 29:1083-94; PMID:19075008; <https://doi.org/10.1128/MCB.01163-08>
- [40] Mahabeleshwar GH, Feng W, Reddy K, Plow EF, Byzova TV. Mechanisms of integrin-vascular endothelial growth factor receptor cross-activation in angiogenesis. *Circ Res* 2007; 101:570-80; PMID:17641225; <https://doi.org/10.1161/CIRCRESAHA.107.155655>
- [41] Paul NR, Jacquemet G, Caswell PT. Endocytic Trafficking of Integrins in Cell Migration. *Curr Biol CB* 2015; 25:R1092-1105; PMID:26583903; <https://doi.org/10.1016/j.cub.2015.09.049>
- [42] Bridgewater RE, Norman JC, Caswell PT. Integrin trafficking at a glance. *J Cell Sci* 2012; 125:3695-701; PMID:23027580; <https://doi.org/10.1242/jcs.095810>
- [43] Morgan MR, Humphries MJ, Bass MD. Synergistic control of cell adhesion by integrins and syndecans. *Nat Rev Mol Cell Biol* 2007; 8:957-69; PMID:17971838; <https://doi.org/10.1038/nrm2289>
- [44] García-Melero A, Reverter M, Hoque M, Meneses-Salas E, Koese M, Conway JRW, Johnsen CH, Alvarez-Guaita A, Morales-Paytuyi F, Elmaghrabi YA, et al. Annexin A6 and Late Endosomal Cholesterol Modulate Integrin Recycling and Cell Migration. *J Biol Chem* 2016; 291:1320-35; <https://doi.org/10.1074/jbc.M115.683557>
- [45] Riggs KA, Hasan N, Humphrey D, Raleigh C, Nevitt C, Corbin D, Hu C. Regulation of integrin endocytic recycling and chemotactic cell migration by syntaxin 6 and VAMP3 interaction. *J Cell Sci* 2012; 125:3827-39; PMID:22573826; <https://doi.org/10.1242/jcs.102566>
- [46] Desgrosellier JS, Cheresh DA. Integrins in cancer: biological implications and therapeutic opportunities. *Nat Rev Cancer* 2010; 10:9-22; PMID:20029421; <https://doi.org/10.1038/nrc2748>
- [47] Nakatsu MN, Davis J, Hughes CCW. Optimized Fibrin Gel Bead Assay for the Study of Angiogenesis. *J Vis Exp JoVE* 2007; e186.